

# Formation of ring-banded spherulites of $\alpha$ and $\beta$ modifications in Poly(butylene adipate)

Jin Liu, Hai-Mu Ye, Jun Xu\*, Bao-Hua Guo

Institute of Polymer Science and Engineering, Department of Chemical Engineering, School of Materials Science and Technology, Tsinghua University, Beijing 100084, China

## ARTICLE INFO

### Article history:

Received 17 June 2011

Received in revised form

23 July 2011

Accepted 1 August 2011

Available online 4 August 2011

### Keywords:

Poly(butylene adipate)

Polymorphism

Ring-banded spherulite

## ABSTRACT

The morphology and crystalline structure of banded spherulites of poly(butylene adipate) (PBA) were investigated by polarized optical microscopy (POM), wide-angle X-ray diffraction (WAXD), atomic force microscopy (AFM) and scanning electronic microscopy (SEM). It was found that after purification and fractionation, the obtained PBA fractions with different molecular weight formed ring-banded spherulites at different temperature ranges. Pure  $\alpha$  and  $\beta$  form of PBA can form regular ring-banded spherulites. AFM and SEM observations of the thin film revealed that the alternative ridges and valleys along the radial direction consisted of edge-on and flat-on lamellae, respectively, indicating the ring-bands in PBA spherulites are the consequence of lamellar twisting. In addition, sequential growth of  $\alpha$  and  $\beta$  form in one PBA spherulite at the same temperature is reported and interpreted by competition of primary nucleation and radial growth of the two crystalline modifications. At a certain temperature range, the  $\alpha$  form PBA has larger primary nucleation rate but lower radial growth rate than the  $\beta$  form PBA, leading to formation of spherulites consisted of  $\alpha$  form at center and  $\beta$  form at the outer region. But finally, a layer of  $\alpha$  form ringless region appears at the outside of the  $\beta$  form ring-banded region before impingement of the neighboring spherulites. These results suggest that besides crystallization temperature, molecular weight has considerable effect on the formation of crystal modification of PBA and the corresponding banded spherulites.

© 2011 Elsevier Ltd. All rights reserved.

## 1. Introduction

Owing to the potential application in environmentally friendly materials, aliphatic biodegradable polymers attract increasing interests in both fundamental and technical research. Their physical properties, such as thermal, mechanical, biodegradable property, largely depend on condensed state as well as chemical structure. Polymorphism is a common phenomenon in aliphatic biodegradable polymers, such as  $\alpha$  and  $\beta$  form in poly[(R)-3-hydroxybutyrate] (PHB) [1],  $\alpha$ ,  $\beta$ ,  $\gamma$  and  $\alpha'$  form in poly(L-lactide) (PLLA) [2,3],  $\alpha$  and  $\beta$  form in poly(butylene succinate) (PBS) [4], which provide an opportunity to adjust and control the physical properties of the bulk material. For instance,  $\beta$  form PHB fiber exhibits higher modulus than its  $\alpha$  form. Thus much attention is concentrated on the detailed structures to understand how polymorphism influences the overall performance. As spherulite is a basic structure inside polymer materials when crystallized from homogeneous melt or solution, the mechanism and morphology of

spherulites has received intensive study in the past decades. Early in the 1950s, Keller utilized polarized optical microscopy (POM) to investigate the mechanism of the morphological features and proposed lamellar twisting model [5–7]. In this model, lamellae orienting along the radii of spherulite twisted as they grew outwards. Eventually, the change of lamellar orientation associated with the change of refraction index, resulting in ring-bands under POM. This model received positive response from Keith and Padden [8], Price [9] at almost the same time. From then on, plenty of efforts have been paid on polymer banded spherulites [10–16]. Various methods have been applied to reveal the organization of the lamellar crystals in ring-banded spherulites. For instance, Xu et al. [15] utilized *in-situ* atomic force microscopy to observe the crystallization of chiral poly[(R)-3-hydroxybutyrate-co-(R)-3-hydroxyhexanoate] (PHBHHx) copolymer, and revealed the twisting details of single lamella. As the research grows deeper and deeper, it is gradually realized that the surface stress accounts for the main drive force of lamellar twisting [16]. Besides the lamellar twisting model, some researchers proposed the rhythmic growth mechanism [11], as observed in poly( $\epsilon$ -caprolactone) (PCL) spherulites [17,18] and poly(bisphenol A hexane ether) [19] crystallized at specific conditions. In that model, the thickness along the radial

\* Corresponding author.

E-mail address: [jun-xu@tsinghua.edu.cn](mailto:jun-xu@tsinghua.edu.cn) (J. Xu).

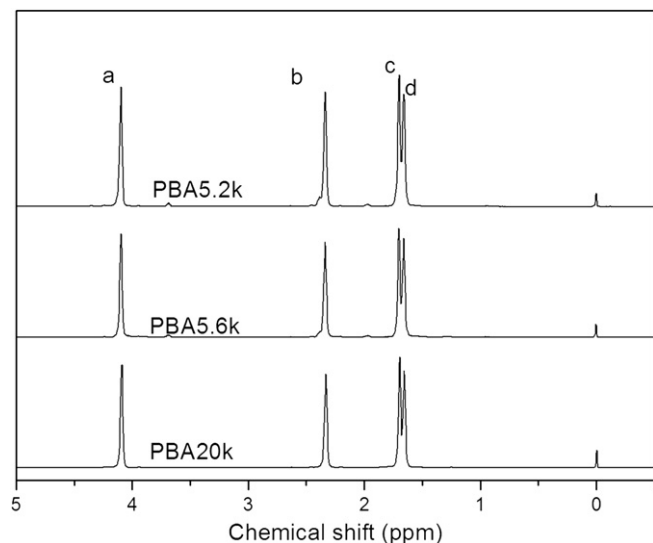


Fig. 1.  $^1\text{H}$  NMR spectra of the three PBA samples.

**Table 1**  
Molecular weights and polydispersity indexes of PBA samples.

	PBA5.2k	PBA5.6k	PBA20k
$M_n$	5200	5600	20400
$M_w$	6600	8100	55900
$M_w/M_n$	1.27	1.45	2.74

direction, owing to the periodic diffusion-induced rhythmic growth, is periodically variable, while the lamellar orientation does not change along the radial direction. However, most of the ring-banded spherulites are revealed to adopt lamellar twisting.

Poly(butylene adipate) (PBA) is a biodegradable polymer with polymorphism. The polymorphism property of PBA determines the

spherulites morphology as well as thermal and enzymatic stability [20–22]. Therefore many works are focusing on controlling PBA polymorphism by blending [23,24], copolymerization [25], or various epitaxial growth conditions [26–30]. However, the relationship between polymorphism and lamellar organization inside the PBA spherulites is not clearly understood yet. In previous work, it was reported that PBA formed  $\alpha$  crystal when isothermally crystallized above 32 °C and  $\beta$  crystal below 27 °C [22,31,32]. When isothermally crystallized at certain temperature between 27 °C and 32 °C,  $\alpha$  and  $\beta$  crystals grew simultaneously and exactly at this temperature range, PBA ring-banded spherulites appeared. It seems that there is some connection between the mixed crystals and ring-banded spherulites in PBA case [22,31], as crystal forms can affect spherulite morphology to some extent. However, there is no other polymer forms ring-banded spherulites like this way. Besides, in another article [33], lamellae in PBA spherulites were believed to protrude outsides without signs of twisting, bending, or turning. In a word, how PBA lamellae organize to form banded spherulites is an unsettled problem owing to the polymorphism and the sensitivity of crystalline structure on temperature.

The purpose of this work is to examine the correlation of temperature, crystal form and ring-banded spherulites in different molecular weight PBA samples. We determined the temperature range for both PBA ring-banded spherulites and mixed crystals, using wide-angle X-ray diffraction (WAXD) and polarized optical microscopy (POM). To verify the cause of ring-bands under POM, we examined the detailed lamellar morphology via atomic force microscopy (AFM) and scanning electron microscopy (SEM). In addition, tilting POM experiment was carried out to analyze whether there is lamellar twisting. Based on the results, we conclude that single crystal form of PBA is capable of generating ring-banded spherulites, resulting from lamellar twisting. Besides, we further analyze the difference of primary nucleation and the radial growth rate between the two crystal modifications and its effect on the ultimate morphology of PBA spherulites.

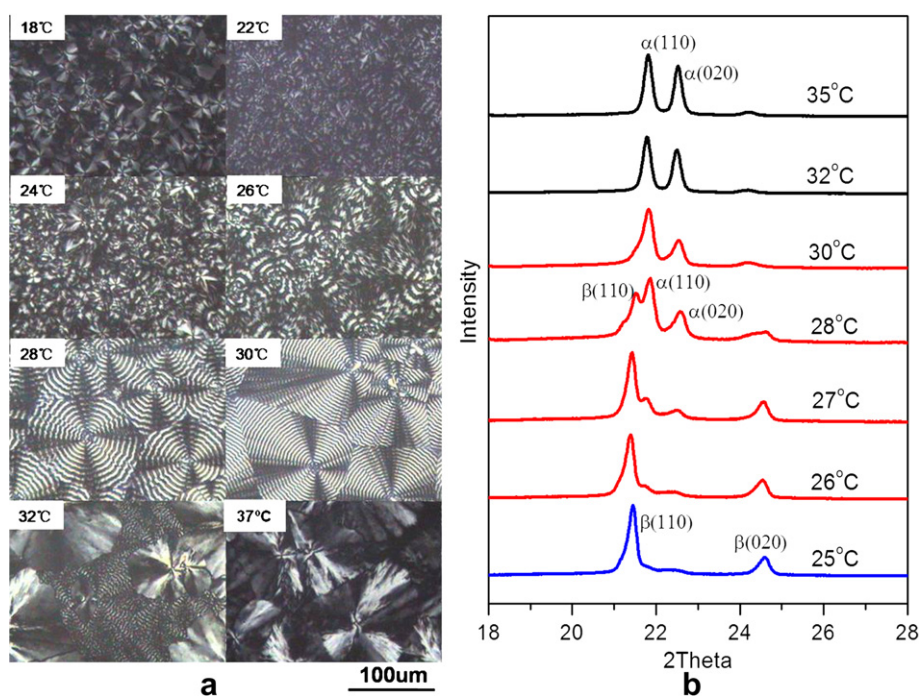
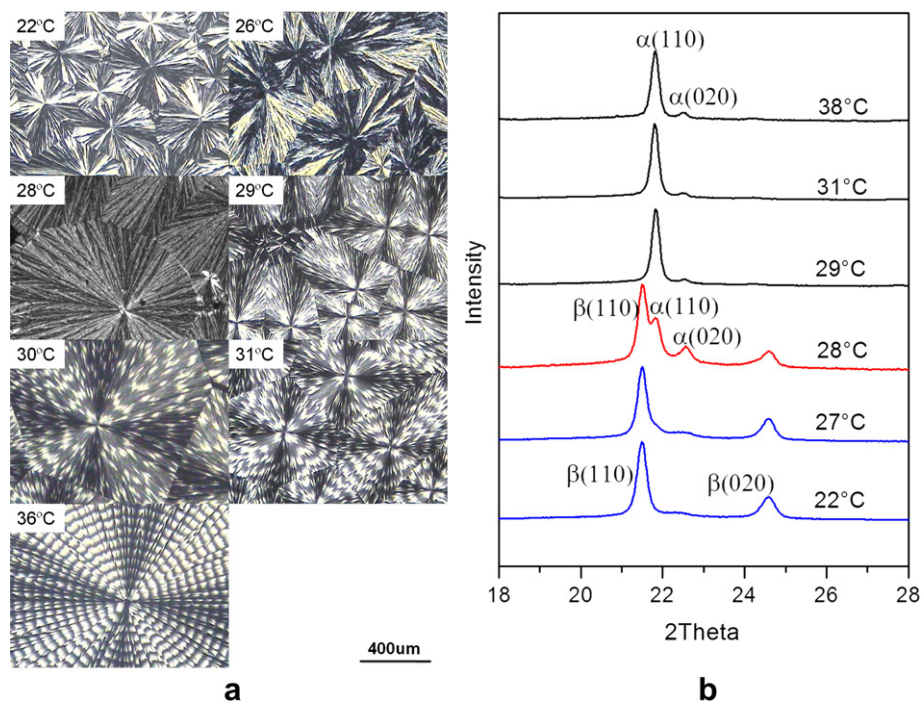


Fig. 2. POM images (a) and WAXD patterns (b) of PBA5.2k after melt-crystallized at different temperatures. The isothermal crystallization temperatures of each sample were marked on the images or curves. Ring-banded spherulites appeared between 26 and 30 °C.



**Fig. 3.** POM images (a) and WAXD patterns (b) of PBA5.6k after melt-crystallized at different temperatures. The isothermal crystallization temperatures of each sample were marked on the images or curves. Ring-banded spherulites appeared above 29 °C.

## 2. Experimental

### 2.1. Materials

Medium molecular weight PBA was synthesized by adipic acid and butylene glycol, using tetra-*n*-butyl-titanate as catalyst [34]. Low molecular weight PBA was purchased from Aldrich Company. To obtain the narrow molecular weight dispersed sample, fractionation

was carried out prior to use. Each PBA sample was purified by precipitation via sequential addition of methanol into the chloroform solution, stored in refrigerator at 4 °C until the white powder deposited onto the bottom. The PBA powder was then dried in vacuum oven at room temperature for 3 days to remove the residual solvent. <sup>1</sup>H NMR spectra of PBA samples were obtained by INOVA NB500 spectrometer at a frequency of 500 MHz, using deuterated chloroform (CDCl<sub>3</sub>) as solvent, and the results are shown in Fig. 1.

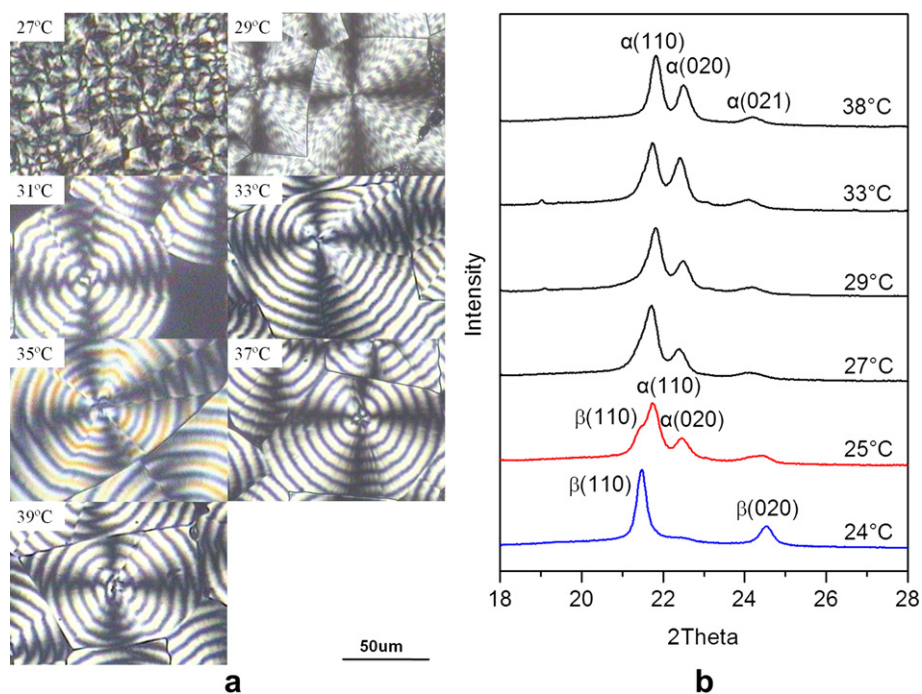


**Fig. 4.** POM images (a) and WAXD patterns (b) of PBA20k after melt-crystallized at different temperatures. The isothermal crystallization temperatures of each sample were marked on the images or curves. Ring-banded spherulites appeared above 29 °C.

**Table 2**  
Crystal forms and the temperature range for ring-banded spherulites of PBA samples.

PBA samples	PBA5.2k	PBA5.6k	PBA26k
$\alpha$ crystal	>30 °C	>28 °C	>27 °C
Mixed crystal	26–30 °C	28 °C	25–27 °C
$\beta$ crystal	<26 °C	<28 °C	<25 °C
Ring-banded	22–32 °C	>29 °C	>29 °C

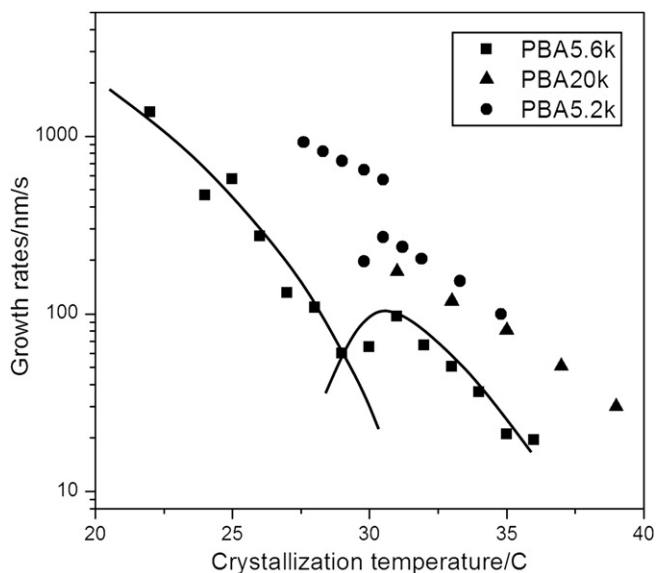


**Fig. 5.** Growth rates of PBA5.6k and PBA20k spherulites as a function of crystallization temperature. Two bell shapes are corresponding to the growth rates of  $\alpha$  crystal and  $\beta$  crystal, respectively.

Molecular weights were determined by gel permeation chromatography (GPC) with a refractive index (RI) detector (Wyatt Optilab rEX) and a PLgel 5  $\mu$ m mixed-D column, using tetrahydrofuran as the eluent and polystyrene as standard material. The measurements were carried out at 25 °C and the eluent flow rate is 1.0 mL/min. The GPC results are displayed in Table 1. PBA5.2k and PBA5.6k are both fractionated from low molecular weight purchased PBA, while PBA20k from medium molecular weight PBA.

## 2.2. Isothermal crystallizations of thin film

Sandwiched between two thin glass slides, PBA powder was placed on a hot stage set at a fixed temperature, i.e. 100 °C in our work, to eliminate the thermal history. After 3 min, PBA sample was transferred onto another hot stage preset at the isothermal crystallization

temperature. Films prepared by this method were characterized by POM, WAXD, AFM and SEM. In order to get an exposed PBA film to conduct the following AFM and SEM experiments, the cover slide was gently removed after complete crystallization.

## 2.3. Characterization

The crystalline structure of PBA samples was characterized by D8 Advanced instrument with Cu K $\alpha$  radiation (3 kW) at a wavelength of 1.542 Å. With a scanning rate of 4°/min and scanning interval of 0.02°, the scanning 2 $\theta$  angle was from 5° to 35° for each sample.

The hot stage for POM observation was placed between crossed polarizer and analyzer, above which equipped with a CCD camera (Panasonic, Japan), enabling to record the whole crystallization process. In order to obtain more information of birefringence, a first order sensitive tint plate (530 nm) was inserted between the sample and analyzer. AFM experiments were performed on SPM-9500J3 (Shimadzu, Japan) under tapping mode. Silicon tips with a resonance frequency of 150 kHz and a spring constant of about 18 N/m were hired. Both the height and phase images were recorded simultaneously. Besides, the inside morphology of spherulites was observed on JSM 7401 scanning electronic microscopy with an accelerating voltage of 30 kV. PBA5.6k spherulite films were etched with solvent vapor of methylamine aqueous solution for 1 h, while PBA20k sample was etched by 36% w/v hydrochloric acid for 10 min. To keep the morphology intact, we carried out SEM experiment without gold sputtering.

## 3. Results and discussion

### 3.1. PBA crystal structure and POM morphology

As both the crystal form and morphology can be influenced by crystallization temperature, it is necessary to check their relationship at first. Figs. 2–4 show the polarized optical images and X-ray diffraction results of three PBA samples. All the PBA fractions can show ringless or ring-banded spherulites, depending on the crystallization temperature, as summarized in Table 2. The different crystal forms were confirmed by WAXD results. Taking PBA5.2k for example, POM images in Fig. 2a show ring-banded spherulites with concentric bands and Maltese cross at the temperature range of 22–32 °C. In addition, the results of WAXD patterns (Fig. 2b) demonstrate that only  $\alpha$  (110) and (020) plane appeared when isothermally crystallized above 30 °C and only  $\beta$  crystal formed below 26 °C. When isothermally crystallized between 26 °C and 30 °C, (110) diffraction plane of  $\alpha$  and  $\beta$  crystal co-existed. From Figs. 3 and 4, it is observed that PBA5.6k crystallized above 28 °C and PBA20k crystallized above 29 °C form ring-banded spherulites, which composed of only  $\alpha$  crystal. These results, demonstrate that the mixed polymorphic crystals are not involved in the formation of ring-banded spherulites of PBA5.6k and PBA20k. The higher

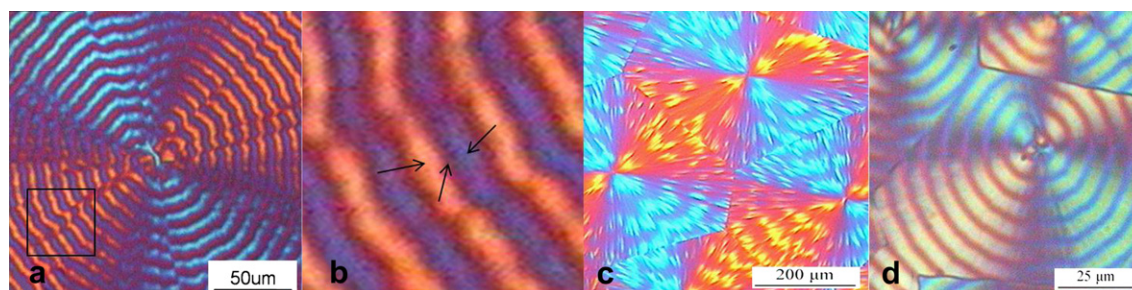


**Fig. 6.** Typical ring-banded spherulites of PBA5.2k (a), PBA5.6k (c), PBA20k (d) and zoom-in image (b) of the area in (a).

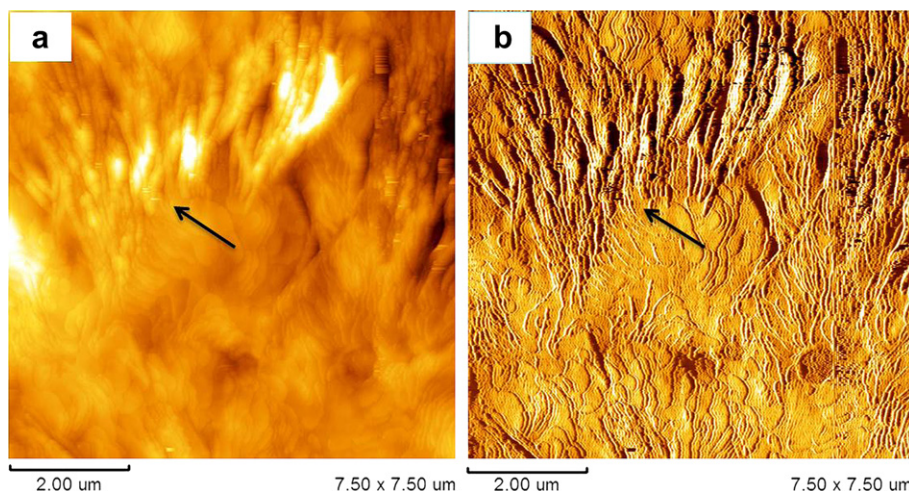


Fig. 7. AFM height (a) and phase (b) image of PBA5.2k spherulite crystallized at 30 °C. The arrow indicates the lamellar twisting area.

crystallization temperature, the more regular ring-bands can be obtained. It is previously suggested that  $\alpha$  crystal is the thermodynamically stable phase, since it shows a higher equilibrium melting point than  $\beta$  form [31]. On the other hand, as shown in Fig. 5, the radial growth rate of PBA5.6k crystal as a function of crystallization temperature seems to be a combination of two bell-shape curves. At lower temperature, the growth rate of  $\beta$  crystal is faster than  $\alpha$  crystal, indicating that the existence of polymorphism is not only determined by thermodynamic stability, but also the growth kinetics. From the above results of the three samples, it seems that both PBA of single crystal and mixed crystals can form ring-banded spherulites; however, as PBA is very sensitive to temperature fluctuation, we need to check it further in the following.

POM and WAXD results of PBA5.2k crystallized at 26 and 28 °C (Fig. 2) seem to be inconsistent: sole morphology was observed from the POM images while the mixed two forms of crystals were revealed by the corresponding WAXD diffractograms. We attribute the seemingly inconsistency to the different thickness of PBA samples used for POM observation and WAXD testing. The sample for WAXD testing must be thick enough, thus there are more primary nuclei of  $\alpha$  crystal per area of the film and the average distance between the neighboring nuclei are shorter so that the total crystallization time is shorter than that in the thin film. As a result, the nuclei of  $\beta$  form crystal did not appear due to the slower nucleation kinetics. Unambiguously, it is revealed that in PBA5.2k sample, the  $\beta$  form crystal can form ring-banded spherulites while the  $\alpha$  form cannot. In contrast, in PBA5.6k and PBA20k samples, the  $\alpha$  form crystal can form ring-banded spherulites.

The above conclusion that different form of crystal accounts for the ring-banded spherulites in different PBA samples can be further confirmed by the sign of the birefringent retardance in POM experiment. There are three principle optical axes in biaxial optical crystal, associated with different refractive indices, labeled by  $n_1$ ,  $n_2$  and  $n_3$  ( $n_1 < n_2 < n_3$ ). Fig. 6 shows the difference of the three PBA samples, i.e. PBA5.2k adopts the texture of double-ringed spherulites, while the other two PBA samples show single-ringed spherulites. It means that  $n_2$  axis is along the radial direction of PBA5.2k double-ringed spherulite and  $n_1$  axis is along the radial direction of the single-ringed spherulite of PBA5.6k and PBA20K. It has been proved that due to comparability of the growth rates along  $a$  and  $b$  axis, single and double-ring areas can be found in one spherulite [35]. In the present case, however, owing to the existence of two crystal forms and the fact that we have not yet observed both single and double-ringed lamellae in one spherulite, we suggest that the

different extinction patterns in ring-banded spherulites are attributed to the different crystal forms.

### 3.2. Lamellar organization in PBA ring-banded spherulites

To demonstrate the cause of ring-banding in PBA spherulites, we applied atomic force microscopy (AFM) to reveal the lamellar

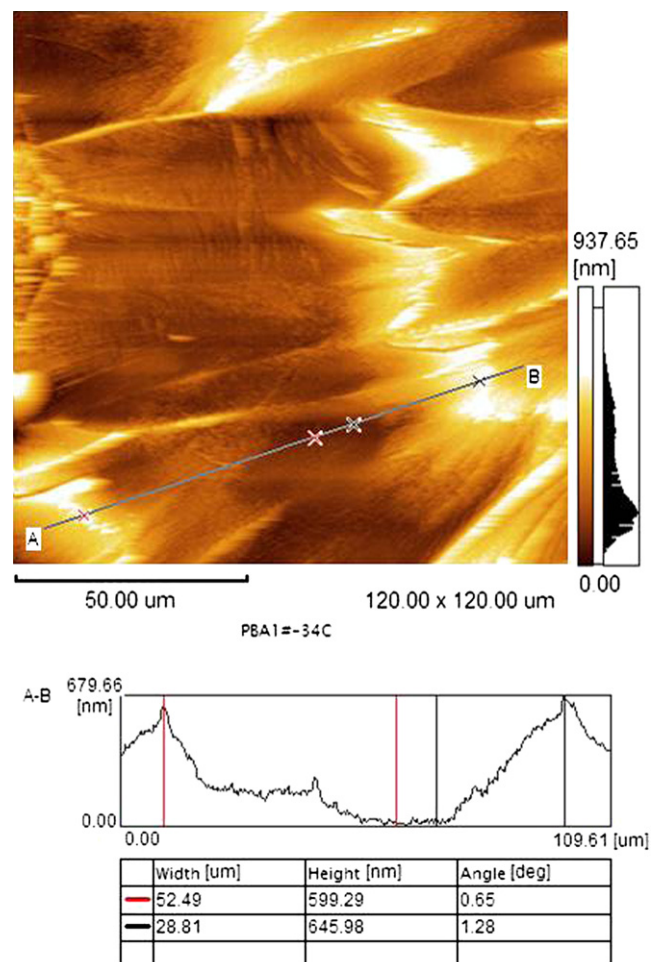
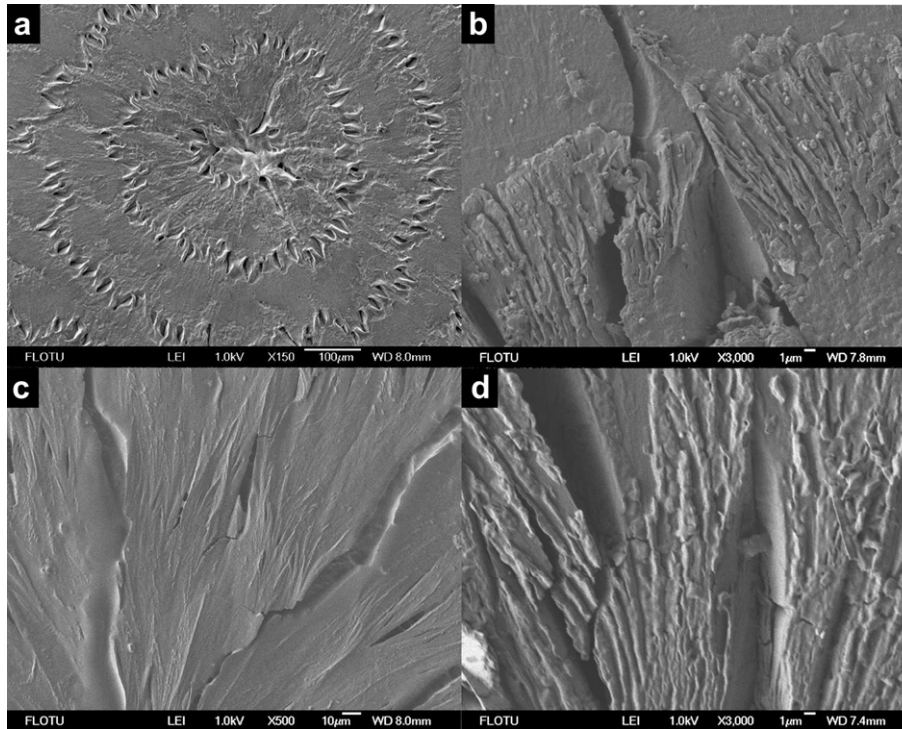


Fig. 8. AFM height image of PBA5.6k isothermally crystallized at 33 °C.



**Fig. 9.** SEM images of PBA5.6k isothermal crystallization at 33 °C, followed by hydrochloric acid etching for 10 min (a) and (b) or methylamine acid etching for 30 min (c) and (d).

organization in the spherulites. As the surface of PBA5.6k and PBA20k spherulites are not smooth enough even in an area of several microns for AFM scanning, SEM was further utilized for characterization of the lamellar morphology.

### 3.2.1. AFM observation of PBA5.2k

Fig. 7 reveals the lamellar morphology in PBA5.2k ring-banded spherulite crystallized at 30 °C (it should be the  $\beta$  form to form banded spherulite). Phase image in Fig. 7b shows that along the radial direction there are two basic lamellar morphologies in each ring-banded spherulite: edge-on and flat-on lamellae. The brighter area in the height image (Fig. 7a) represents the ridge area of the spherulite surface, which is composed of edge-on lamellae. Correspondingly, the valley area is filled by flat-on lamellae. The two different lamellar orientations arouse diversity of refractive index when observed under POM, presenting alternative concentric bands. The transition between edge-on and flat-on lamellae is observed, indicated by the arrow in Fig. 7. Our results demonstrate that single crystal form of PBA5.2k can generate ring-banded spherulites by

lamellar twisting, which differs from a previous paper, where no sign accounting for PBA lamellar twisting was reported [33].

### 3.2.2. SEM observation of PBA5.6k

PBA5.6k exhibits larger band spacing which is distinctively different from the other PBA samples. To rule out the possibility of rhythmic growth with periodic variation of thickness along radial direction, we examined the global height difference in the spherulite. Cross section of AFM height image (Fig. 8) shows the height difference in the ring-banded spherulite is about 700 nm, which is much smaller than the total thickness of the sample (about 10 μm). The mere thickness variation of 700 nm is not sufficient to cause bands of such strong birefringence contrast between ridge and valley. In contrast, the rhythmic banded spherulites of PCL grown from the solution with constant concentration show the height difference of several microns, almost comparable to the film thickness [18].

To verify the lamellar orientation in PBA5.6k spherulites, the etched surface was further examined by SEM experiment. The SEM

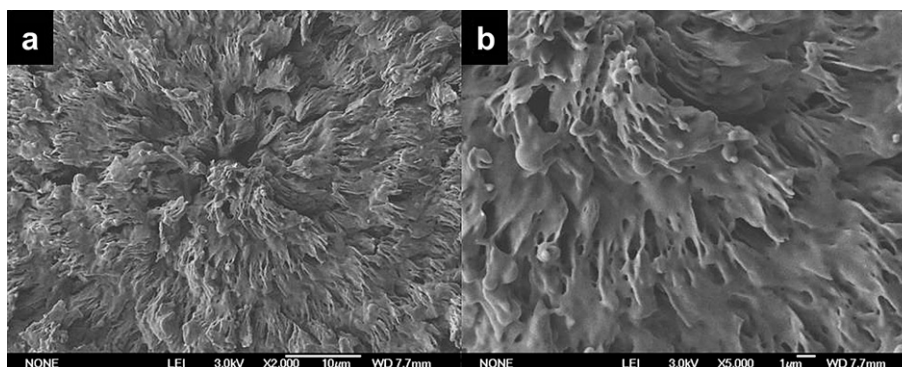


**Fig. 10.** SEM images of PBA20k isothermal crystallization at 33 °C, followed by hydrochloric acid etching for 10 min.

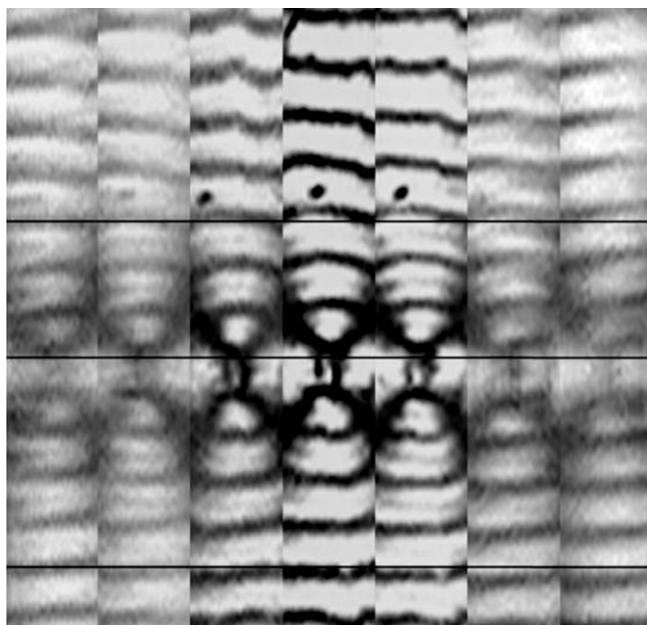


**Fig. 11.** POM images of ring-banded spherulite of PBA20k film tilted from  $-30^\circ$  (left) to  $30^\circ$  (right) with an interval of  $10^\circ$ . Vertical shift of bands indicates the lamellar twisting within the spherulites.

images of PBA5.6k ring-banded spherulites crystallized at  $33^\circ\text{C}$  ( $\alpha$  crystal) show that the band spacing is about  $100\ \mu\text{m}$ , in agreement with the POM observation (Fig. 3). Similar to PBA5.2k, PBA5.6k spherulites composed of two different lamellar morphologies alternatively along the radial direction (Fig. 9). It is worth noting that the edge-on lamellae region is easier to be eroded than the flat-on lamellae region, as methylamine acid may penetrate more easily into the space between the edge-on lamellae (Fig. 9c and d). Due to the compact packing of lamellae, the connection between the edge-on and flat-on lamellae is not clear. However, as we have already known that PBA5.6k crystallized at this temperature compose of single crystal form (Table 2), we can conclude that the ring-banded spherulites of PBA5.6k can be attributed to the change of lamellar orientation.

Fig. 9c shows that the lamellae of PBA5.6k are lath shaped, while those of PBA5.2k (Fig. 7b) are similar to the hexagonal morphology of the PBA  $\alpha$  form crystal previously observed [36,37]. The more straightforward lamellae in PBA5.6k spherulites indicate faster growth rate of (110) plane than that of (020) plane, leading to the

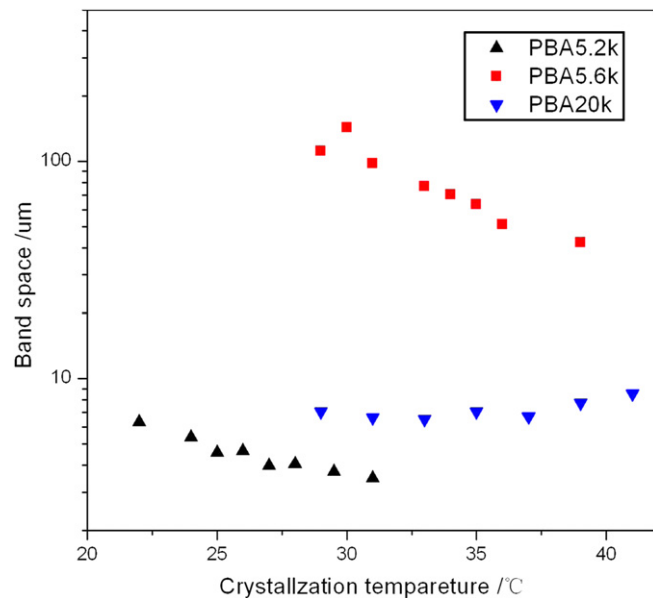


**Fig. 13.** Ring-banded spacing in spherulites of the three samples crystallized at different temperatures.

stronger intensity of (110) peak than (020) peak. In contrast, the growth rate of (110) plane in PBA5.2k is comparable to that of (020) plane, causing similar intensity of (110) and (020) planes.

### 3.2.3. SEM observation of PBA20k

The PBA20k sample was etched with hydrochloric acid for 10 min before SEM observation. As presented in Fig. 10, PBA20k spherulites isothermally crystallized at  $33^\circ\text{C}$  ( $\alpha$  crystal) shows ring-banded morphology when observed under SEM. The zoom-in image (Fig. 10b) clearly identifies the change of lamellar orientation during the growth process. Consequently, the change of lamellar orientation is responsible for the ring-band of PBA20k spherulites.

Tilting experiment was further carried out to verify the lamellar twisting mechanism in PBA ring-banded spherulites. This method was originally adopted by Keith and Padden [8] to investigate polyethylene spherulites and then adopted by other researchers [35,38,39]. Supposing a twisted lamella as a screw, the extinction feature of each band will shift when rotates around the lamella itself, which can be used to judge the existence of lamellar twisting in PBA samples. Fig. 11 clearly reveals the shift of bands within the PBA20k spherulite, indicating existence of lamellar twisting.

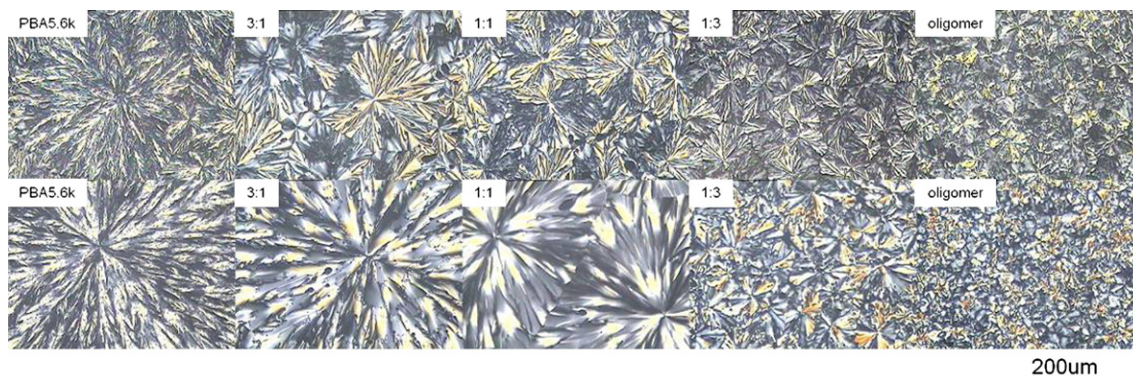


**Fig. 12.** POM images of PBA5.6k and PBA oligomer blends. The blends are crystallized at (from up to down)  $27$  and  $35^\circ\text{C}$ . The relatively ratios between the two fractions are 1:0, 3:1, 1:1, 1:3, 1:0 (from the left column to the right).

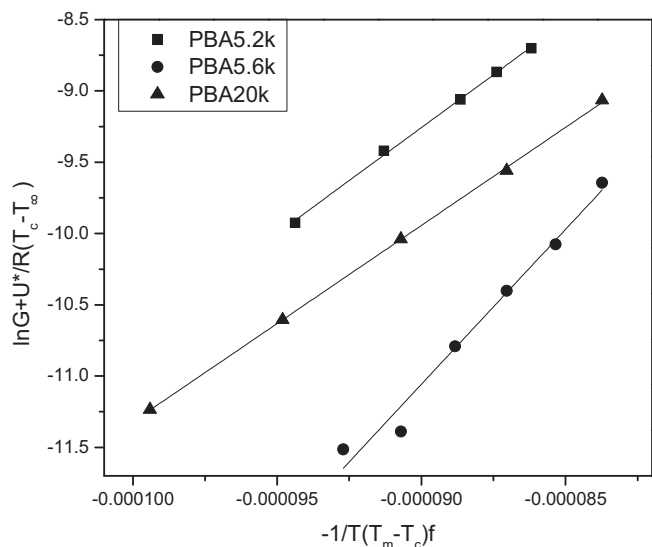


Fig. 14. The plot of  $\ln(G) + U^*/R(T_c - T_\infty)$  vs.  $-1/T_c(\Delta T)f$ .

Furthermore, we note that the bands on the top of the spherulite center shift upwards while those at the bottom shift downward, which suggest that the two parts have the opposite twisting senses. This agrees with the previous report [40] that both twisting senses were observed in the same PCL spherulite and confirms our twisting scheme of lamellae in the ring-banded spherulites of achiral polymers (Fig. 9b in literature [41]).

### 3.3. Mechanism of PBA ring-banded spherulites

In summary, though the three PBA samples have the same molecular structure and merely differ in molecular weight, they

display different crystallization features. First of all, ring-banded spherulites appear at different temperature ranges, i.e., PBA5.6k and PBA20k show ring-banded spherulites at higher crystallization temperature when  $\alpha$  modification forms, while PBA5.2k exhibits ring-banded morphology at lower crystallization temperature with  $\beta$  form crystal. According to the lamellae twisting model, ring-banded morphology in spherulites requires a stack of lamellae to twist cooperatively. From the POM images of PBA5.2k  $\alpha$  form crystal (the bottom right image of Fig. 2a), or PBA5.6k  $\beta$  form crystal (the top two images in Fig. 3a), we can observe the alternation of birefringence intensity, implying the occurrence of lamellae twisting. However, owing to lacking cooperation among the lamellae, it is difficult to exhibit regular ring-banded morphology on the whole spherulite.

What's more, primary nucleation density is another significant factor to influence the appearance of ring-banded spherulites. Considering the relatively small spherulites of PBA5.2k and PBA20k crystallized at low temperatures in Figs. 2a and 4a, we could not judge whether the two samples have the ability to form ring-banded spherulites at the low temperature range. To investigate what factors affect the primary nucleation density, we blend PBA5.6k sample, which could generate large spherulites at all temperatures, with PBA oligomer that exhibit small spherulites to observe the spherulite morphology crystallized at certain temperatures and the result is shown in Fig. 12. In general, the size of PBA spherulites became smaller from left to right, suggesting the primary nucleation density increased with the increase of PBA oligomer ratio. Closer observation reveals that the blends crystallized at higher temperature, i.e. 35 °C, exhibited the morphology similar to PBA5.6k ring-banded spherulites so long as the weight ratio of PBA oligomer remained below 50%. This phenomenon suggests PBA5.6k plays a major role by profiling the main frame of the PBA spherulites and cutting down the density of primary nucleation. On the other hand, we notice that band spacing became wider with the addition of PBA oligomer, indicating the incorporated PBA oligomer was helpful to release the surface stress of

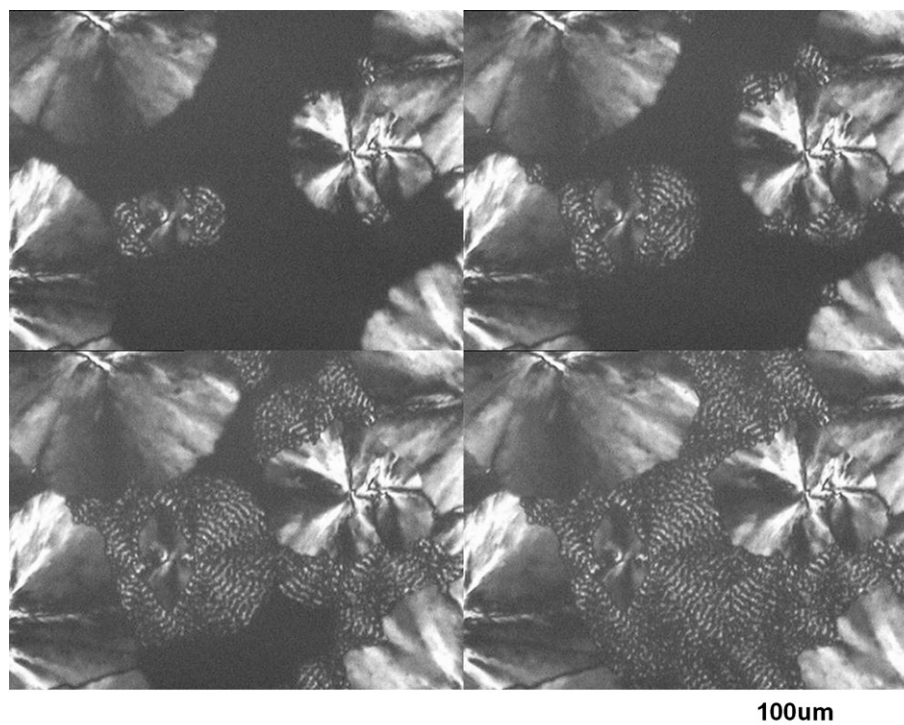


Fig. 15. In-situ crystallization of PBA5.2k isothermally crystallized at 32 °C. Ring-banded morphology emerged at the edge of ringless morphology.

lamellae. However, how the PBA5.6k fraction decreases the density of primary nucleation and the PBA oligomer influences the ring-band spacing are still under investigation.

Variation of the band spacing with temperature is presented in Fig. 13. Band spacing in PBA5.2k and PBA5.6k samples decrease with crystallization temperature while that in PBA20k remains constant. This is a rare situation comparing to other polymers, which usually demonstrate larger band spacing at higher temperature [15,38]. In addition, the band spacing in PBA5.6k (about 50–100 μm) is much larger than that in PBA5.2k and PBA20k (about 4–10 μm). According to Owen's equation on single twisted lamella [42], band spacing  $P$  can be related to surface stress  $\sigma$ , the azimuth angle  $\theta$  between the fold direction and the growth direction, the elastic modulus  $E$  and the lamellar thickness  $t$  as follow

$$P = \left(\frac{2}{3}\right)^{1/2} \pi \sin \theta \cos \theta \left(\frac{E}{\sigma}\right)^{1/2} t^{3/2} \quad (1)$$

It is reasonable to assume that the elastic modulus  $E$  of the lamellae remains constant regardless of variance of crystallization temperature. Besides, as pointed out previously [41], the surface stress  $\sigma$  decreases with increasing crystallization temperature. Lamellar thickness  $t$  increases with crystallization temperature

[31]. The two factors will lead to enhanced band spacing with increasing temperature; however, this is not the case. Therefore, the azimuth angle  $\theta$  of the surface stress has to be considered as another possible factor to influence the band spacing. We suppose that the azimuth angle  $\theta$  of surface stress will shift accordingly when the crystallization temperature arises, leading to smaller band spacing.

To evaluate the activation energy of secondary crystallization in PBA samples, Hoffman–Lauritzen equation [43] is adopted:

$$G = G_0 \exp\left[-U^*/R(T_c - T_\infty)\right] \exp\left[-K_g/T(\Delta T)f\right] \quad (2)$$

where  $G$  is the radial growth rate of the spherulite,  $U^*$  is the activation energy of the segmental movement,  $T_\infty$  is the temperature where segmental movement ceases and is usually taken 30 K below the glass transition temperature ( $T_g = -61^\circ\text{C}$ ) [34],  $\Delta T = T_m^0 - T_c$  is the supercooling,  $f$  is the correction factor and has the form of  $f = 2T_c/T_m^0 + T_c$ , and  $K_g$  the kinetic parameter related to the free energy of fold surface and lateral surface as the following:

$$K_g = \frac{nb\sigma\sigma_e T_m^0}{\Delta h_f k_B} \quad (3)$$

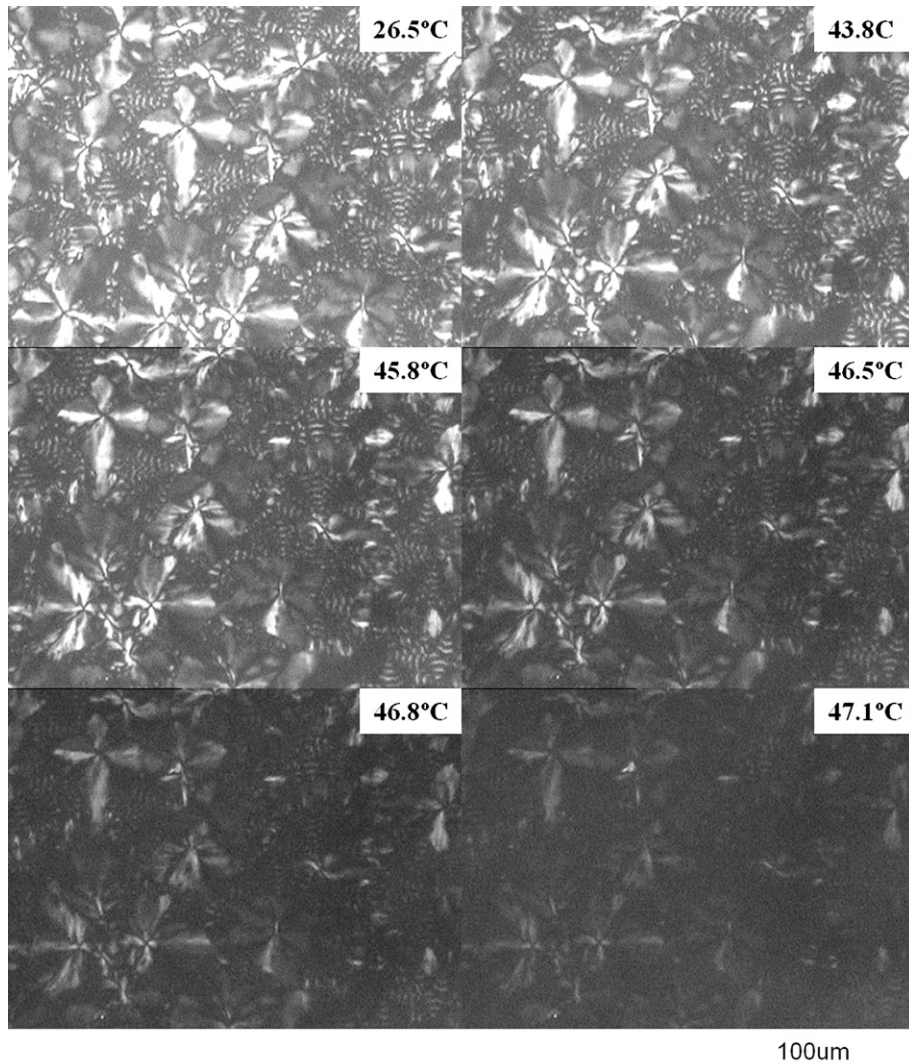
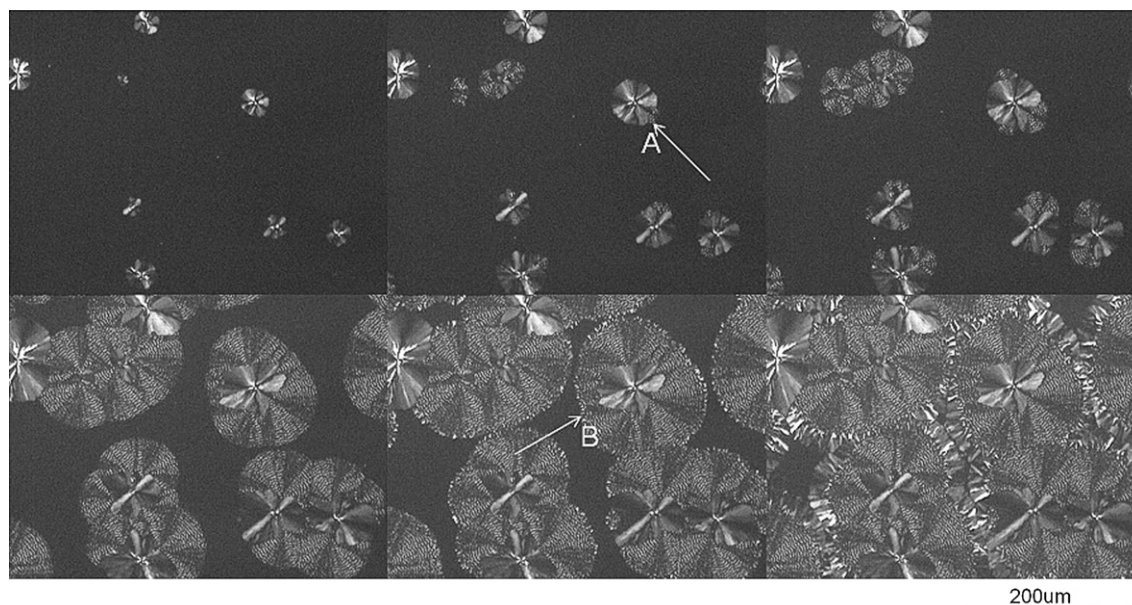


Fig. 16. In-situ melting of PBA5.2k spherulites crystallized at 32 °C. Ringless and ring-banded regions melt at different temperature. The core region with higher melting temperature corresponds to the final melting point in Fig. 1 of Ref [31] which is transformed in the heating process.



**Fig. 17.** Sequential growth of the two crystal modifications in PBA5.2k spherulite at 30 °C, from ringless to ring-banded then back to ringless morphology. Arrow A indicates the region of banded  $\beta$  crystal nucleation at the edge of ringless  $\alpha$  crystal. Arrow B indicates the second transition, nucleation of  $\alpha$  crystal at the periphery of  $\beta$  crystal.

As the three PBA samples have the same chemical constitution, it is reasonable to assume that they have the same activation energy for diffusion (assuming  $U^*$  is 1.5 kcal mol<sup>-1</sup> or 6.28 kJ mol<sup>-1</sup>) [43]. By this mean,  $K_g$  for  $\alpha$  crystal can be obtained from the slope of the plot of  $\ln(G) + U^*/R(T_c - T_\infty)$  vs.  $-1/T_c(\Delta T)f$  and we get 148 000, 217 000 and 138000 K<sup>2</sup> for the PBA5.2k, PBA5.6k and PBA20k, respectively (Fig. 14). We attribute the difference of growth rates to the diversity of activation energy for formation of secondary nuclei. PBA5.6k has much higher  $K_g$  value, causing slower radial growth rate than the other samples, as observed in Fig. 5. Besides, the different  $K_g$  values indicate that the main growth faces are different among the samples, as is consistent with the discussion in Section 3.2.2.

### 3.4. Competitive growth of polymorphic crystals at the same crystallization temperature

It is noticed that mixed crystals can be formed at intermediate isothermal crystallization temperatures. PBA5.2K spherulites crystallized at 32 °C show both ringless and ring-banded morphologies in the same spherulite (Fig. 15). The primary nuclei of the ringless spherulites emerge prior to those of the ring-banded spherulites. When the ringless spherulites grow to some extent, several nuclei of ring-banded spherulites appear at the edge of the ringless spherulites, indicating that the crystal structure of ring-banded spherulites is different from that of ringless spherulites. Otherwise, lamellae of ring-banded spherulites would begin to grow at the whole periphery of ringless spherulites. Besides, these two distinct morphologies melt at different temperatures in heating test (Fig. 16). The ring-banded region melts prior to the ringless region, which suggests the different crystal forms in the two morphologies. Therefore, the above results suggest that the ringless spherulites are composed of  $\alpha$  crystal, while the ring-banded spherulites are of  $\beta$  crystal form. Sometimes, two transitions of the spherulite morphology could be observed, ringless to ring-banded transition and ring-banded to ringless transition along the radial direction, as shown in Fig. 17.

Sequential growth of polymorphic crystals in one PBA spherulite has already been examined by Woo et al. [44], via changing the crystallization temperature. In our work, however, the sequential growth of the two forms of crystal in the spherulite happened at the

same crystallization temperature. Consequently, there are other factors to influence the competition of the polymorphic crystals besides crystallization temperature. One is the relative rate of the formation of primary nuclei and the radial growth rate. The spherulite center consists of  $\alpha$  crystals, indicating that they have larger primary nucleation rate than  $\beta$  crystals. The corresponding growth rates of the three growth regions are presented in Fig. 18. The growth rate of ring-banded region is 0.615  $\mu\text{m/s}$ , much larger than that of the two ringless regions (about 0.288 and 0.168  $\mu\text{m/s}$ ). Therefore, the ring-banded region encircles the inner ringless center as the spherulite grows larger and larger.

Another important factor affecting the competitive growth of the two modifications lies in the molecular weight distribution of the sample, especially for the low molecular weight fraction. The

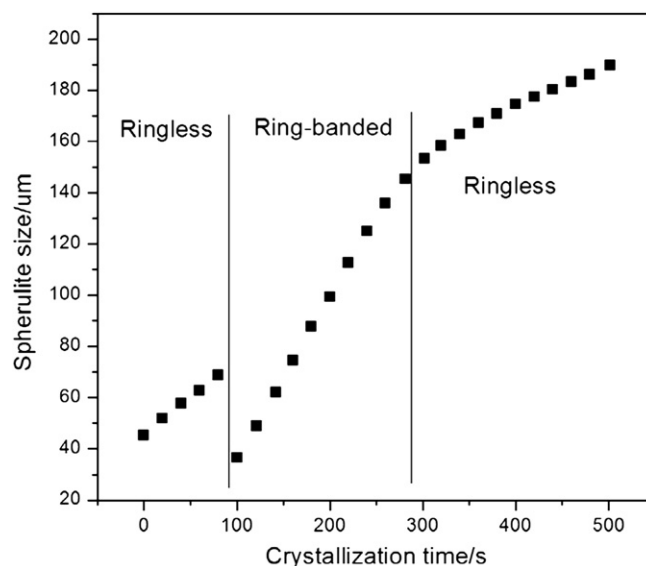


**Fig. 18.** Various grow rates of the ringless and ring-banded region of PBA5.2k spherulite crystallized at 30 °C, calculated from Fig. 17.

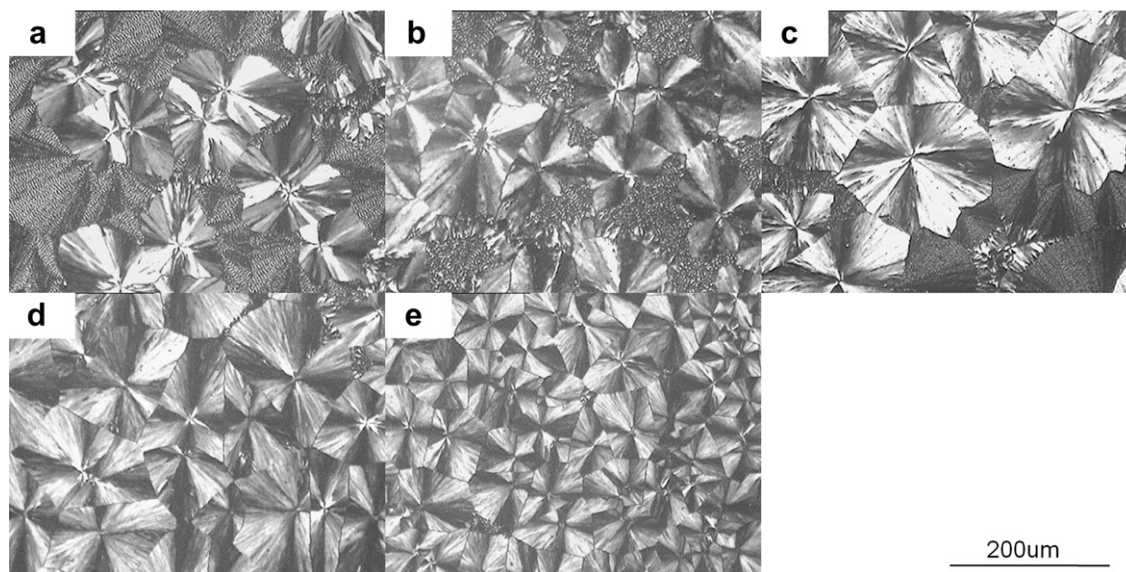


**Fig. 19.** Crystallization of PBA spherulites degraded from PBA5.2k. The spherulites were crystallized at 30 °C after holding on a hot stage set at 180 °C temperature for (a) 3 min, (b) 10 min, (c) 20 min, (d) 40 min, (e) 60 min. The relative small spherulite size with increasing holding time indicates that degraded PBA fraction favors the primary nucleation of  $\alpha$  crystal.

second transition, from banded  $\beta$  crystals to ringless  $\alpha$  crystals can be attributed to variation of the molecular weight of the crystallized PBA chains. During crystallization, the low molecular weight polymer chains will be enriched at the growth front in the melt. The low molecular weight fraction in PBA5.2k owns a lower melting point and thus the crystallization window of the  $\beta$ -form crystals will shift to a lower temperature, assuming the same supercooling needed for the coexistence of the polymorphic crystals. As a result, low molecular weight fraction of PBA tends to form  $\alpha$  crystal when isothermally crystallized at the same temperature.

To further prove the idea that molecular weight can shift the coexistence temperature window of the two forms of PBA crystals, we examined the crystallization behavior of relative low molecular weight PBA degraded from PBA5.2k by holding it at 180 °C for different periods of time. At the high temperature, it is expected that PBA would degrade to smaller molecular weight as the holding time increases. The results in Fig. 19 demonstrate that PBA5.2k spherulites exhibit larger fraction of ringless morphology after holding at 180 °C (Fig. 19 (a)–(c)) than that obtained at the same crystallization temperature without degradation at 180 °C (Fig. 18). By extending degradation time to 40 or 60 min (Fig. 19d and e), the ring-banded morphology disappears completely and spherulites become smaller in size, confirming that the degraded PBA with lower molecular weight favor the primary nucleation of  $\alpha$  crystal.

#### 4. Conclusions

PBA fractions with different molecular weights and polydispersity indices were prepared to investigate the mechanism of PBA ring-banded spherulites. POM and WAXD results demonstrate that single crystal form ( $\alpha$  or  $\beta$ ) of PBA can generate ring-banded spherulites.  $\beta$ -form spherulites of PBA5.2k sample show double-ringed spherulite, in which the birefringent retardance changes the sign at the neighboring bands. In contrast,  $\alpha$  form spherulites of PBA5.6k and PBA20k sample demonstrate single-ringed spherulite, in which the birefringent retardance is negative. For the same  $\alpha$  form, PBA5.6k and PBA20k fraction reveal quite different dependence of band spacing on the crystallization temperature. PBA5.6k sample has a much higher energy barrier to form the secondary nuclei than

PBA20k, leading to a much lower radial growth rate of the spherulites of the former. The detailed morphologies observed under SEM and AFM confirm that the change of lamellar orientation is responsible for the formation of ring-banded spherulites in the three PBA samples. PBA5.2k spherulites crystallized at 30 °C consist of three layers: ringless  $\alpha$  form, ring-banded  $\beta$  form and the final ringless  $\alpha$  form. The results show that at this temperature,  $\alpha$  form has higher primary nucleation rate and lower radial growth rate than the  $\beta$  form. Our experimental results suggest that the final morphology of PBA spherulites is affected by the rate of nucleation and the radial growth of  $\alpha$  and  $\beta$  crystals. The primary nucleation rate will influence the morphology at the center of the spherulite, as it can determine which form of crystal will grow first; while the secondary nucleation rate will determine the morphology of the outside region in the spherulites. Growth of PBA spherulites may also be a process of separation of different molecular weight polymer chains. PBA chains with higher molecular weight will crystallize first and the fractions with lower molecular weight crystallize at last. The latter is favorable to form  $\alpha$  crystal compared with the higher molecular weight fraction when crystallized under the same temperature.

#### Acknowledgments

This work was supported by the National Natural Science Foundation of China (Grant Nos. 50673050 and 20974060). We are grateful to Professor Zhi-Hua Gan for fruitful discussions.

#### References

- [1] Pazar RJ, Hocking PJ, Raymond S, Marchessault RH. *Macromolecules* 1998; 31(19):6585–92.
- [2] Kalb B, Pennings AJ. *Polymer* 1980;21(6):607–12.
- [3] Hoogsteen W, Postema AR, Pennings AJ, ten Brinke G, Zugenmaier P. *Macromolecules* 1990;23(2):634–42.
- [4] Ichikawa Y, Kondo H, Igarashi Y, Noguchi K, Okuyama K, Washiyama J. *Polymer* 2000;41(12):4719–27.
- [5] Keller A. *Journal of Polymer Science* 1955;17(84):291–308.
- [6] Keller A. *Journal of Polymer Science* 1955;17(85):351–64.
- [7] Keller A, Waring JRS. *Journal of Polymer Science* 1955;17(86):447–72.
- [8] Keith HD, Padden FJ. *Journal of Polymer Science* 1959;39(135):101–22.
- [9] Price FP. *Journal of Polymer Science* 1959;39(135):139–50.
- [10] Bassett DC, Hodge AM. *Polymer* 1978;19(4):469–72.

- [11] Kyu T, Chiu HW, Guenther AJ, Okabe Y, Saito H, Inoue T. *Physical Review Letters* 1999;83(14):2749–52.
- [12] Toda A, Arita T, Hikosaka M. *Polymer* 2001;42(5):2223–33.
- [13] Keith HD. *Polymer* 2001;42(25):9987–93.
- [14] Bassett DC. *Journal of Macromolecular Science-Physics* 2003;B42(2):227–56.
- [15] Xu J, Guo BH, Zhang ZM, Zhou JJ, Jiang Y, Yan S, et al. *Macromolecules* 2004;37(11):4118–23.
- [16] Lotz B, Cheng SZD. *Polymer* 2005;46(3):577–610.
- [17] Wang Z, Hu Z, Chen Y, Gong Y, Huang H, He T. *Macromolecules* 2007;40(12):4381–5.
- [18] Wang ZB, Alfonso GC, Hu ZJ, Zhang JD, He TB. *Macromolecules* 2008;41(20):7584–95.
- [19] Wang Y, Chan C-M, Li L, Ng K-M. *Langmuir* 2006;22(17):7384–90.
- [20] Gan ZH, Abe H, Doi Y. *Macromolecular Chemistry and Physics* 2002;203(16):2369–74.
- [21] Gan ZH, Kuwabara K, Abe H, Iwata T, Doi Y. *Polymer Degradation and Stability* 2005;87(1):191–9.
- [22] Zhao L, Wang X, Li L, Gan Z. *Polymer* 2007;48(20):6152–61.
- [23] Yang J, Pan P, Hua L, Zhu B, Dong T, Inoue Y. *Macromolecules* 2010;43(20):8610–8.
- [24] Yang JJ, Pan PJ, Hua L, Xie YH, Dong T, Zhu B, et al. *Polymer* 2011;52(15):3460–8.
- [25] Zhao L, Gan Z. *Polymer Degradation and Stability* 2006;91(10):2429–36.
- [26] Kai W, Zhu B, He Y, Inoue Y. *Journal of Polymer Science Part B-Polymer Physics* 2005;43(17):2340–51.
- [27] Sun Y, Li H, Huang Y, Chen E, Zhao L, Gan Z, et al. *Macromolecules* 2005;38(7):2739–43.
- [28] Wu MC, Woo EM. *Polymer International* 2005;54(12):1681–8.
- [29] Dong T, Kai W, Inoue Y. *Macromolecules* 2007;40(23):8285–90.
- [30] Jiang N, Zhao L, Gan Z. *Polymer Degradation and Stability* 2010;95(6):1045–53.
- [31] Gan Z, Kuwabara K, Abe H, Iwata T, Doi Y. *Biomacromolecules* 2004;5(2):371–8.
- [32] Woo EM, Wu MC. *Journal of Polymer Science Part B-Polymer Physics* 2005;43(13):1662–72.
- [33] Fromsdorf A, Woo EM, Lee LT, Chen YF, Forster S. *Macromolecular Rapid Communications* 2008;29(15):1322–8.
- [34] Zorba T, Chrissafis K, Paraskevopoulos KM, Bikiaris DN. *Polymer Degradation and Stability* 2007;92(2):222–30.
- [35] Ye HM, Xu J, Guo BH, Iwata T. *Macromolecules* 2009;42(3):694–701.
- [36] Pouget E, Almontassir A, Casas MT, Puiggali J. *Macromolecules* 2003;36(3):698–705.
- [37] Iwata T, Kobayashi S, Tabata K, Yonezawa N, Doi Y. *Macromolecular Bioscience* 2004;4(3):296–307.
- [38] Maillard D, Prud'homme RE. *Macromolecules* 2008;41(5):1705–12.
- [39] Meyer A, Yen KC, Li S-H, Forster S, Woo EM. *Industrial and Engineering Chemistry Research* 2010;49(23):12084–92.
- [40] Nozue Y, Hirano S, Kurita R, Kawasaki N, Ueno S, Iida A, et al. *Polymer* 2004;45(25):8299–302.
- [41] Ye HM, Wang JS, Tang S, Xu J, Feng XQ, Guo BH, et al. *Macromolecules* 2010;43(13):5762–70.
- [42] Owen AJ. *Polymer* 1997;38(14):3705–8.
- [43] Hoffman JD, Davis GT, Lauritzen JI. *Crystalline and noncrystalline solids*. In: *Treatise on Solid State Chemistry*, vol. 3. New York: Plenum Press; 1976. p. 497–614.
- [44] Woo EM, Yen KC, Wu MC. *Journal of Polymer Science Part B-Polymer Physics* 2008;46(9):892–9.